Int J Biometeorol (2010) 54:13–22
DOI 10.1007/s00484-009-0247-y

# Modeling effects of urban heat island mitigation strategies on heat-related morbidity: a case study for Phoenix, Arizona, USA

**Humberto R. Silva · Patrick E. Phelan · Jay S. Golden**

Received: 4 January 2009 / Accepted: 1 July 2009 / Published online: 26 July 2009


**Abstract** A zero-dimensional energy balance model was previously developed to serve as a user-friendly mitigation tool for practitioners seeking to study the urban heat island (UHI) effect. Accordingly, this established model is applied here to show the relative effects of four common mitigation strategies: increasing the overall (1) emissivity, (2) percentage of vegetated area, (3) thermal conductivity, and (4) albedo of the urban environment in a series of percentage increases by 5, 10, 15, and 20% from baseline values. In addition to modeling mitigation strategies, we present how the model can be utilized to evaluate human health vulnerability from excessive heat-related events, based on heat-related emergency service data from 2002 to 2006. The 24-h average heat index is shown to have the greatest correlation to heat-related emergency calls in the Phoenix (Arizona, USA) metropolitan region. The four modeled UHI mitigation strategies, taken in combination, would lead to a 48% reduction in annual heat-related emergency service calls, where increasing the albedo is the single most effective UHI mitigation strategy.

**Keywords** Health vulnerability · Heat wave · Urban heat island · Morbidity · Emergency medical dispatch · Numerical modeling

H. R. Silva · P. E. Phelan
Department of Mechanical and Aerospace Engineering,
Arizona State University,
Tempe, AZ, USA

H. R. Silva · P. E. Phelan · J. S. Golden
National Center of Excellence on SMART Innovations,
Arizona State University,
Tempe, AZ, USA

J. S. Golden (✉)
School of Sustainability, Arizona State University,
P.O. Box 875502, 800 South Cady Mall Room # 356,
Tempe, AZ 85287-5502, USA
e-mail: Jay.Golden@asu.edu

## Introduction

There is indeed a dearth of simple, easy to use, inexpensive and validated urban energy balance models. The relatively complex urban energy models in the literature include the Weather Research and Forecasting Model (WRF; Michalakes et al. 1998), the fifth-generation Pennsylvania State University—National Center for Atmospheric Research Mesoscale Model (MM5; Grossman-Clarke et al. 2005), and Envi-Met (2008). All of these models require extensive training and/or knowledge of atmospheric sciences, physics and computational sciences. Although these models have been shown to be validated for many cases and have researchers continuously pushing development to more advanced capabilities, they exist largely for usage by highly trained scientific researchers. In an effort to create a more user-friendly model for governmental agency officials, previous work by Silva et al. (2008) successfully showed that one can create a computationally inexpensive and simple-to-use model that is validated versus a more robust model such as MM5. The following analysis will apply this relatively simple model to investigate how various urban heat island (UHI) mitigation strategies reduce the number of heat-related emergency dispatch calls for the Phoenix (Arizona, USA) metropolitan area.

## Mitigation strategies

### Model recap

Beginning in the fashion of Golden et al. (2005), we can represent the energy flows for an urban volume by six major components. Keeping intact the surface energy balance while simultaneously simplifying a very complex problem, one can express the following governing equation

**Table 1** Modeled baseline urban thermophysical property values for the Phoenix metropolitan area (Bhardwaj et al. 2006; Grossman-Clarke et al. 2005; Taha et al. 2000; Pomerantz et al. 1997; Rosenfeld et al. 1995)

| Classification | Baseline area share | Albedo | Emissivity | Thermal Conductivity [W $m^{-1}$ $K^{-1}$] |
|---|---|---|---|---|
| Roof | 0.184 | 0.200 | 0.850 | 0.062 |
| Road | 0.140 | 0.150 | 0.890 | 1.400 |
| Sidewalk | 0.030 | 0.300 | 0.850 | 1.000 |
| Parking area | 0.143 | 0.150 | 0.890 | 1.000 |
| Soil | 0.189 | 0.300 | 0.945 | 1.120 |
| Vegetation | 0.304 | 0.200 | 0.945 | 0.670 |
| Water | 0.011 | 0.080 | 0.945 | 0.600 |
| Baseline value | | 0.206 | 0.909 | 0.802 |

for the lumped urban temperature (Bhardwaj et al. 2006; Silva et al. 2008):

$$mc\frac{dT}{dt} = (1-\alpha)q_{sol}A + q_{anthro}A - q_{cond}A - q_{evap}A - q_{conv}A - q_{rad}A \quad (1)$$

where $m$ is mass, $c$ specific heat, $t$ time, $\alpha$ albedo, $A$ area, $q_{\mathrm{sol}}$ the incident time-dependent solar heat flux, $q_{\mathrm{anthro}}$ the anthropogenic heat flux, $q_{\mathrm{evap}}$ the evapotranspiration heat flux, $q_{\mathrm{cond}}$ the conductive heat loss to the deep ground, $q_{\mathrm{conv}}$ the outgoing convective heat flux, $q_{\mathrm{rad}}$ the outgoing emitted radiative heat flux, and $T$ the characteristic temperature. Dividing through by $A$ and transforming the formula to a finite difference scheme ready for numerical implementation yields:

$$T^{n+1} = T^n + \frac{\Delta t}{\rho\, c\, \delta\, x}\left[(1-\alpha)q^n_{sol} + q^n_{anthro} - q^n_{cond} - q^n_{evap} - q^n_{conv} - q^n_{rad}\right] \quad (2)$$

where $\rho$ is density, and $\delta x$ the distance between the surface and the measured 50.8-cm (20-inch) ground temperature, $\Delta t$ the time step, the superscript $n$ represents the present time step, and the superscript $n$+1 represents the future time step.

Utilizing the same methodologies as in Silva et al. (2008), the characteristic urban temperature $T$ can finally be expressed as:

$$T^{n+1} = T^n\left[1 - \frac{\Delta t}{\rho\, c\, \delta x}\left(h^n_{conv} + h^n_{rad} + \frac{k_{grd}}{\delta x}\right)\right] + \frac{\Delta t}{\rho\, c\, \delta x}\left[h^n_{conv}T^n_{air(Rural)} + h^n_{rad}T^n_{sky} + \frac{k_{grd}}{\delta x}T_{grd}\right] + \frac{\Delta t}{\rho\, c\, \delta x}\left[(1-\alpha)q^n_{Sol} + q^n_{Anthro} - E_{t0}\,\rho_{H_20}\,h_{fg}\right] \quad (3)$$

where $k_{\mathrm{grd}}$ is the thermal conductivity of the ground, $T_{\mathrm{grd}}$ the ground temperature measured at a depth of 50.8 cm (20 inches; AZMET 2008), $E_{\mathrm{t0}}$ the measured evapotranspiration (in meters) for vegetated areas, $h_{\mathrm{fg}}$ the latent heat of vaporization for water, $\rho_{\mathrm{H_2O}}$ the density of water, $T_{air(\mathrm{Rural})}$ the measured rural dry-bulb air temperature, $h_{\mathrm{conv}}$ the convection heat transfer coefficient, $h_{\mathrm{rad}}$ the radiation heat transfer coefficient, and $T_{\mathrm{sky}}$ the "sky" temperature, i.e., the effective temperature of the sky with respect to emitted radiation (ASHRAE 2004). Note that the variables $q^n_{anthro}$, $h^n_{rad}$, $T^n_{sky}$, $h^n_{conv}$ have embedded terms. Equation 3 is the model that will be applied to all analysis in this manuscript. All of the meteorological data needed in Eq. 3 are taken from AZMET (2008), and the anthropogenic heat data are taken from EIA (2008) via the formulation of Sailor and Lu (2004). As discussed in the next section, we will show the formulation of the radiation coefficient term below since one of its parameters (emissivity $\varepsilon$) will be perturbed in our mitigation scheme. The $h_{\mathrm{rad}}$ term changes with each time step and is given by (at a particular time step; Cengel 2003):

$$h_{rad} = \varepsilon\sigma\frac{\left(T^4 - T^4_{sky}\right)}{\left(T - T_{sky}\right)} \quad (4)$$

where $\sigma$ is the Stefan-Boltzmann constant.

## Perturbed values

There are four values embedded in Eq. 3 that will be explored for UHI mitigation purposes, and to determine which mitigation strategies lead to an overall greater percent decrease in the calculated characteristic 24-h average temperature. The four investigated UHI mitigation strategies increase the overall: (1) emissivity ($\varepsilon$ embedded in the $h^n_{rad}$ term), (2) percentage of vegetated area (the weight of the $E_{\mathrm{t0}}$

**Table 2** Corresponding changes in thermophysical property baseline values when the percentage of vegetated area is increased by 5, 10, 15, and 20%

| Increase in vegetated area | Volumetric Heat Capacity [$10^6$ J $m^{-3}$ $K^{-1}$] | Emissivity | Albedo | Thermal Conductivity [W $m^{-1}$ $K^{-1}$] |
|---|---|---|---|---|
| 5% | 2.079 | 0.909 | 0.206 | 0.801 |
| 10% | 2.054 | 0.911 | 0.206 | 0.800 |
| 15% | 2.029 | 0.911 | 0.207 | 0.799 |
| 20% | 2.004 | 0.912 | 0.207 | 0.798 |

**Table 3** Modeled baseline and increased urban thermophysical property values for the Phoenix metropolitan area, for exploring the four urban heat island (UHI) mitigation strategies

| | Increase in emissivity | Increase in fraction of vegetated area | Increase in thermal conductivity [W $m^{-1}$ $K^{-1}$] | Increase in albedo |
|---|---|---|---|---|
| BASELINE | 0.909 | 0.304 | 0.802 | 0.206 |
| 5% | 0.954 | 0.319 | 0.842 | 0.216 |
| 10% | 0.999 | 0.334 | 0.882 | 0.227 |
| 15% | — | 0.349 | 0.922 | 0.237 |
| 20% | — | 0.365 | 0.962 | 0.247 |

term), (3) thermal conductivity of the ground ($k_{grd}$), and (4) albedo ($\alpha$) of the urban environment. The idea is to run the model with these above four values increased from their baseline values (Bhardwaj et al. 2006; Grossman-Clarke et al. 2005; Taha et al. 2000; Pomerantz et al. 1997; Rosenfeld et al. 1995) at various percentages (see Tables 1, 2, 3). The values are increased by 5, 10, 15, and 20% (5% increments) from their baseline values over a physically reasonable range (up to 20%, 10% for emissivity). For the emissivity ε, note that ε can only be increased by 10% as its value at this point is already 0.999. This value of ε=0.999 is the maximum value of ε applied for all UHI mitigation strategies. In addition to examining how increases in these individual parameters lead to reductions in urban characteristic temperature, we also examine how all of these mitigation strategies change the temperature when implemented in unison.

For simplicity, as the percentage of vegetated area is increased, we do not consider any corresponding increase in the relative humidity. Our range of vegetation percentage modifications yielded a small change in overall relative humidity given our classification scheme (see Table 1) and for the range of typical temperature and dew point temperatures in Phoenix. For example, a straightforward psychometric calculation involving the partial pressure of water vapor and the saturated vapor pressure of the air in our control volume (Phoenix urban area from the ground to the 2 m height at which air temperature is measured through AZMET) we can achieve a maximum 5% change in relative humidity for typical temperatures in Phoenix (AZMET 2008) year round in 2008. Also, we will treat other alterations brought on by the thermophysical constants on each other as negligible. However, changing the percent vegetated area does alter the other model inputs as presented in Table 2.

The values in Table 2 were calculated by increasing the vegetated area to the desired value, while uniformly reducing all the other six area classifications. Specifically, we adopt a seven area classification scheme approach (Bhardwaj et al. 2006; shown in Table 1) where one of the classifications was vegetation. All seven classifications have a percent share of the entire Phoenix urban area. First, we increased the vegetation classification percentage share by the desired amount (5, 10, 15, or 20%) and then reduced the other six classifications percentage shares' uniformly so the sum added up to 1. Then, we took this new percentage share value for each classification and multiplied it by its respective parameter value (albedo, emissivity, thermal conductivity, or volumetric heat capacity) and took the weighted average over the entire Phoenix urban area to yield the new value for each individual parameter. To better illustrate this process, see the example for the albedo change for a 20% increase in vegetated area (Table 4).

## Effects on average urban temperature

Figure 1 and Table 5 indicate how each UHI mitigation strategy leads to decreases in the calculated characteristic temperature *T*. It is seen from Fig. 1 that increasing the overall albedo has the strongest influence on the 24-h average urban characteristic temperature. This is because solar radiation drives the energy balance. Increasing the emissivity

**Table 4** Corresponding detailed change in the albedo baseline value when the percentage of vegetated area is increased (modified) by 20%

| Classification | Fraction of baseline area | Albedo value | Baseline albedo contribution | Modified fraction of baseline area | Modified albedo contribution |
|---|---|---|---|---|---|
| Roof | 0.184 | 0.200 | 0.037 | 0.174 | 0.035 |
| Road | 0.140 | 0.150 | 0.021 | 0.130 | 0.020 |
| Sidewalk | 0.030 | 0.300 | 0.009 | 0.020 | 0.006 |
| Parking area | 0.143 | 0.150 | 0.021 | 0.133 | 0.020 |
| Soil | 0.189 | 0.300 | 0.057 | 0.179 | 0.054 |
| Vegetation | 0.304 | 0.200 | 0.061 | 0.365 | 0.073 |
| Water | 0.011 | 0.080 | 0.001 | 0.001 | 0.000 |
| Total sum | 1.000 | | 0.206 | 1.000 | 0.207 |

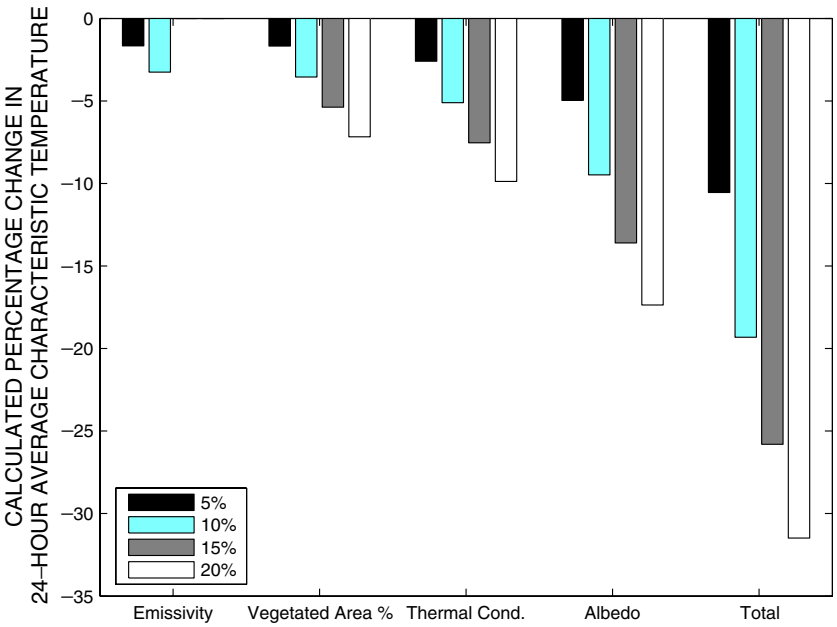


**Fig. 1** Calculated percentage change in 24-h average characteristic urban temperature for the listed urban heat island (UHI) mitigation strategies for the Phoenix metropolitan area. Each mitigation strategy (except emissivity) is increased by 5, 10, 15, and 20%

has the smallest effect overall. This makes sense since the emissivity of the Phoenix urban fabric is already high (0.91), thus limiting any further increases. Also, increasing the thermal conductivity has a greater effect than increasing the percentage of vegetated area. This is due to the fact that the percentage of vegetated areas (~0.3–0.37) is outweighed by the rest of the urban environment, so we can conclude that the thermal conductivity strategy should have a greater effect than increasing the vegetated area strategy as most of the urban area is not covered by vegetation.

The combined mitigation strategy effect (All four strategies included; Table 5), where we increase all of the four respective parameters by the maximum 20% over their baseline values, can reduce the overall temperature by almost 32% as predicted by the model. This is a theoretical finding as increasing these values may be difficult to implement due to financial and time constraints (even though the increases yield physically reasonable values). It is better to concentrate merely on albedo, because the share of albedo in the reduction of 24-h average urban characteristic is highest. Implementation of these mitigation strategies may be achieved by changing the material of urban roads to yield higher albedo by e.g., increased use of concrete pavements or whitetopping of existing pavements (Golden and Kaloush 2006). Surface treatments and paints can provide positive adjustments of material emissivity values. A thermal conductivity strategy can include the inclusion of metallic or ceramic particles to the pavement/sidewalk material mix, thus yielding higher thermal conductance (Mityakin and Pivinskii 1980). Rooftop mitigation strategies include white rooftops and/or green rooftops that incorporate membrane separation of the roof with the topmost layer incorporating vegetation and soil. A common mitigation strategy is the deployment of an urban forestation program, which increases the percentage of vegetated area in the urban environment by adding more trees, grass, succulents, etc. (EPA 2001, 2008). Figure 2 recasts the data of Fig. 1 to highlight the relative contributions of each mitigation strategy to the reduction in the predicted 24-h average urban characteristic temperature.

**Table 5** Percentage decrease in calculated 24-h average characteristic temperature resulting from the four UHI mitigation strategies

| | Increase in emissivity | Increase in fraction of vegetated area | Increase in thermal conductivity | Increase in albedo | All four strategies included |
|---|---|---|---|---|---|
| 5% | -1.66% | -1.68% | -2.60% | -4.97% | -10.55% |
| 10% | -3.25% | -3.55% | -5.11% | -9.48% | -19.32% |
| 15% | — | -5.38% | -7.54% | -13.59% | -25.81% |
| 20% | — | -7.18% | -9.88% | -17.36% | -31.48% |

## Correlation with heat-related morbidity

### Correlation analysis and extended validation

We have taken into consideration nine different sets of meteorological data for correlation to heat-related emergency calls between 2002 and 2006 in the greater Phoenix AZ region (Golden et al. 2008). They include: (1) 24-h average heat index (relates temperature and relative humidity to give a true felt outside temperature), (2) 24-h average relative humidity, (3) 24-h average temperature, (4) 24-h maximum heat index, (5) 24-h maximum

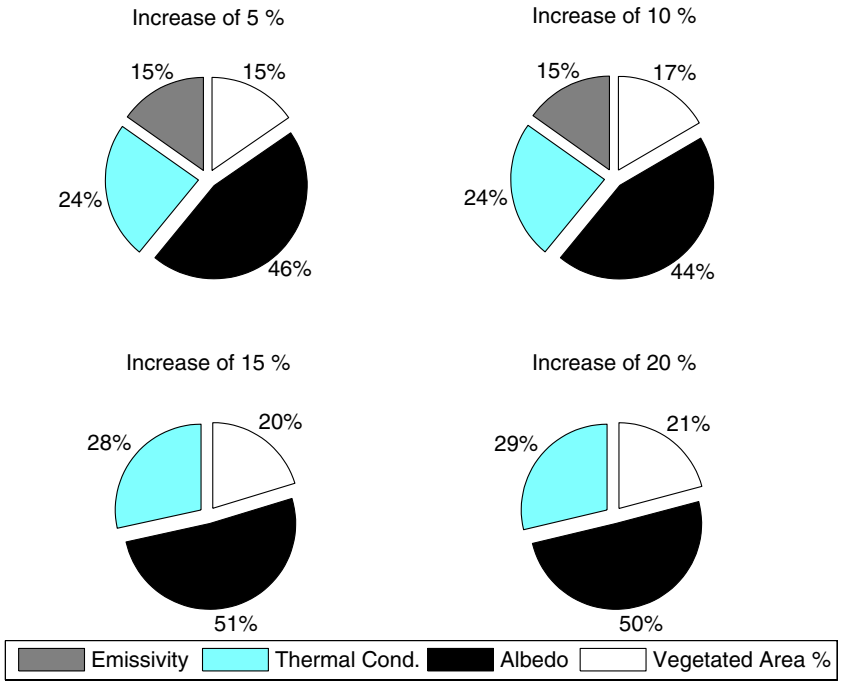


**Fig. 2** Pie graph describing the relative contributions of the four UHI mitigation strategies to the reduction in 24-h average urban characteristic temperature

relative humidity, (6) 24-h maximum temperature, (7) 24-h minimum heat index, (8) 24-h minimum relative humidity, and (9) 24-h minimum temperature as shown in Fig. 3. Statistically, as presented by Golden et al. (2008) these indicate that either 24-h maximum temperature or 24-h average heat index has the strongest correlation to calls for service during this time frame.

We use the classic correlation analysis as presented by Kreyszig (1999), which can be used for matrices or vectors of the same size:

$$r = \frac{\sum_m \sum_n (A_{mn} - \overline{A})(B_{mn} - \overline{B})}{\sqrt{\left[\left(\sum_m \sum_n (A_{mn} - \overline{A})^2\right)\right]\left[\left(\sum_m \sum_n (B_{mn} - \overline{B})^2\right)\right]}} \quad (5)$$

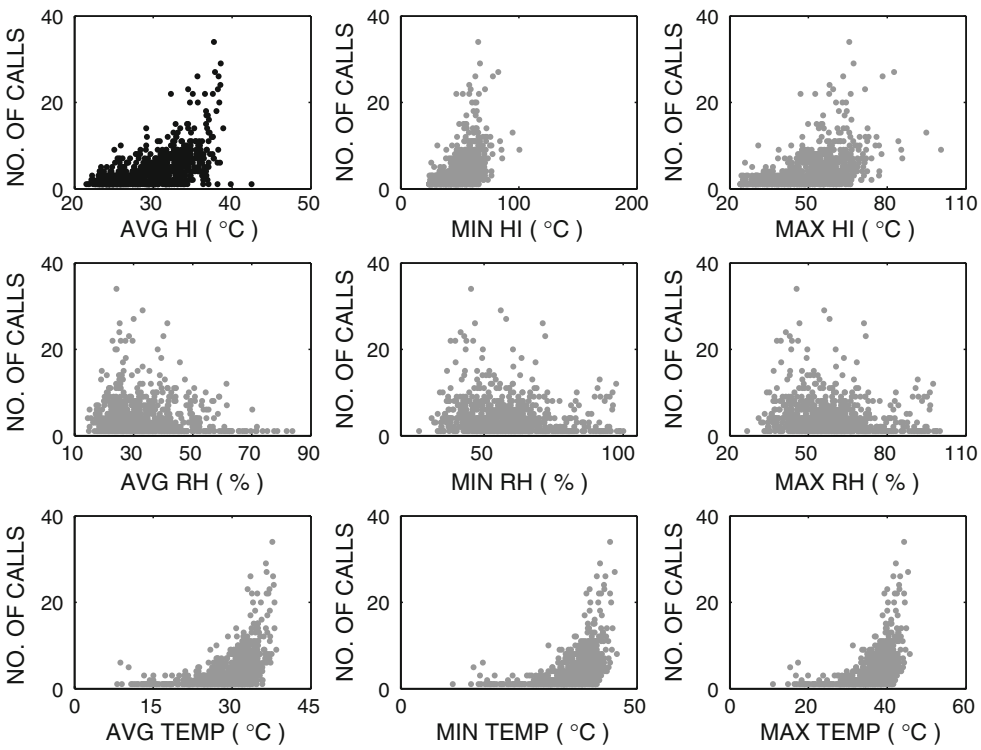


**Fig. 3** Scatter plots of nine different meteorological data sets against the number of heat-related emergency calls for the city of Phoenix spanning 2002–2006. *AVG* 24-h average, *MIN* 24-h minimum, *MAX* 2 4-h maximum, *HI* heat index, *RH* relative humidity, *TEMP* Temperature, *# OF CALLS* number of heat-related emergency calls

**Table 6** Correlation values between Phoenix heat-related emergency calls (2002—2006) and meteorological data

| | Correlation value |
|---|---|
| 24-h average heat index | 0.56 |
| 24-h average temperature | 0.51 |
| 24-h minimum temperature | 0.50 |
| 24-h maximum heat index | 0.47 |
| 24-h maximum temperature | 0.46 |
| 24-h minimum heat index | 0.34 |
| 24-h maximum relative humidity | -0.17 |
| 24-h average relative humidity | -0.11 |
| 24-h minimum relative humidity | -0.01 |

where $A$ and $B$ are the two sets of data that are being compared, where $\overline{A}$ and $\overline{B}$ are the means (averages) of their respective data set.

These meteorological data sets (except for ones involving the heat index) were all obtained from AZMET (2008) and were extracted in accordance with the day of the year that the call occurred. The data sets were taken from the AZMET measurements at their Phoenix Encanto (urban) and Queen Creek (rural) stations for this study. Also, these data sets would have been extracted in accordance with the time of day the call occurred and would have allowed for more meteorological data sets to be considered (including temperature at time of call, heat index at time of call, relative humidity at time of call, etc.) but the data provided for the heat-related emergency calls did not provide such detail. The heat index was calculated with the measured air temperature and relative humidity data via the following equation (Stull 1999):

$$HI = \begin{bmatrix} 1 \\ T \\ T^2 \\ T^3 \end{bmatrix} \begin{bmatrix} 16.92 & 5.38 & 7.29(10)^{-3} & 2.92(10)^{-5} \\ 1.85(10)^{-1} & -1.00(10)^{-1} & -8.15(10)^{-4} & 1.97(10)^{-7} \\ 9.42(10)^{-3} & 3.45(10)^{-4} & 1.02(10)^{-5} & 8.43(10)^{-10} \\ -3.86(10)^{-5} & 1.43(10)^{-6} & -2.18(10)^{-8} & -4.82(10)^{-11} \end{bmatrix} \begin{bmatrix} 1 & R & R^2 & R^3 \end{bmatrix} \quad (6)$$

where $HI$ is the heat index, $T$ the temperature (in degrees Fahrenheit), and $R$ the relative humidity (in percentage). To solve for all the data points, Eq. 6 needs to be repeated for the entire data set and can be solved symbolically with a linear algebra solver or by matrix multiplication $\left[HI = T_i \mathrm{A}_{ij} R_j\right]$ if implemented numerically.

After all of our calculations were completed for the entire set of emergency calls, we found that the highest

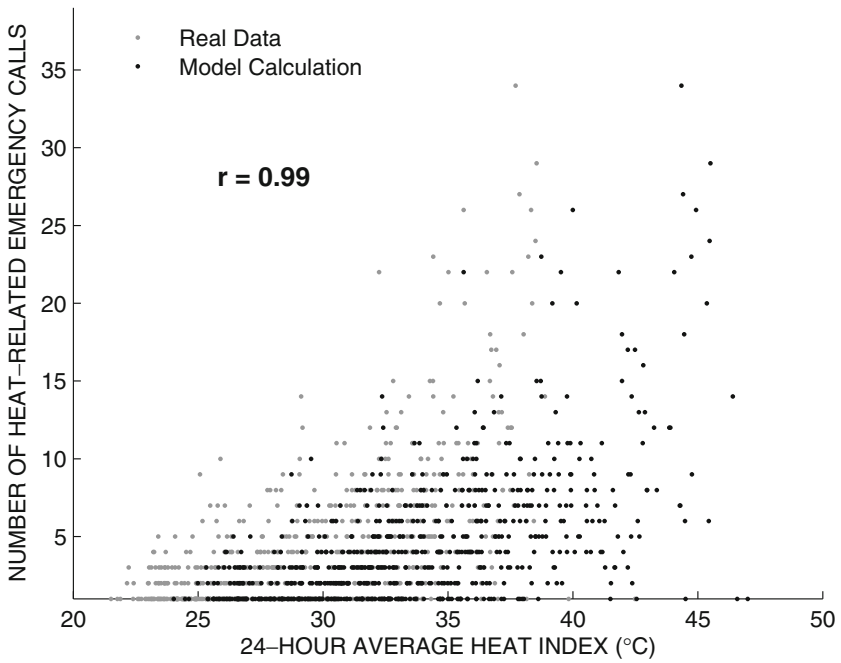


**Fig. 4** Scatter plot of the actual 24-h average heat index and the modeled 24-h average heat index with their associated occurrences of the number of heat-related emergency calls for the city of Phoenix spanning 2002–2006

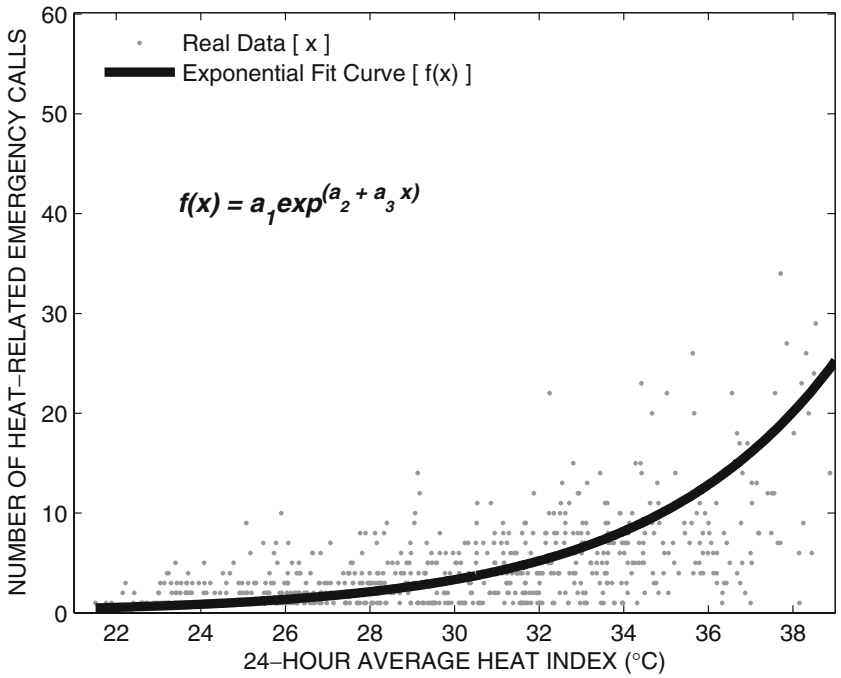


**Fig. 5** Exponential fit curve of the actual 24-h average heat index and associated occurrences of the number of heat-related emergency calls for the city of Phoenix spanning 2002-2006 with $a_1$=12.20, $a_2$=-−2.04, and $a_3$=0.13, where $x$ is the 24-h average heat index in °C

correlation to the heat-related emergency calls was that of the 24-h average heat index, at a value of $r$=0.56 as shown in Table 6. Next, we show that the model predicts a relatively similar 24-h average heat index as compared to the measured 24-h average heat index at the time of the heat-related call. In order to do this we run the model for the entire 5-year period, then extract the temperature as predicted by the model in accordance with the day of the year for each year with each emergency call and then calculate the 24-h average heat index via Eq. 6. Figure 4 demonstrates graphically that the model is in strong agreement with the actual raw data at the occurrence of their respective heat-related call. In fact, the two data sets (the actual 24-h average heat index and the calculated 24-h average heat index from the model) have nearly a perfect correlation, with $r$=0.99 via Eq. 5.

**Table 7** Predicted average annual reduction in Phoenix heat-related emergency calls, where the total annual average number of heat-related emergency calls is 637

| | Increase in emissivity | Increase in percent vegetated areas | Increase in thermal conductivity | Increase in albedo | All four strategies included |
|---|---|---|---|---|---|
| 5% | 16 | 17 | 25 | 48 | 103 |
| 10% | 32 | 35 | 50 | 92 | 188 |
| 15% | — | 53 | 73 | 132 | 251 |
| 20% | — | 70 | 96 | 169 | 306 |

## Exponential fit curve analysis

After validating our model with highest correlated meteorological data sets to heat-related emergency calls in the city of Phoenix region, we developed a methodology for using the model to predict reductions in the number of these calls as a result of implementing UHI mitigation strategies. We use the raw data in conjunction with model predictions to bring this analysis together. Given a discrete and raw data set (24-h average heat index) we can create a continuous curve that accurately portrays the typical behavior for this discrete data set. From the previous plots it is observed that the raw data behave nonlinearly in an exponential fashion. Thus, we utilize an exponential function that behaves similarly to the raw data set. Many different types of exponential functions were experimented with but the one with the highest correlation will be discussed below. There are many factors and anomalies that can disrupt the correlation with such a raw data set, especially similar to the discrete jumps in Fig. 5. However, the correlation for the chosen exponential function was still 0.60, showing a strong relationship between the two data sets. The chosen exponential function was the following:

$$f(x) = a_1 \exp^{(a_2 + a_3 x)} \tag{7}$$

where $a_1$=12.20, $a_2$=−12.04, and $a_3$=0.13 as shown in Fig. 5 superimposed on top of the raw data. We utilized this function in combination with the model to predict the decrease in heat-related emergency calls when UHI mitigation strategies are put into effect.

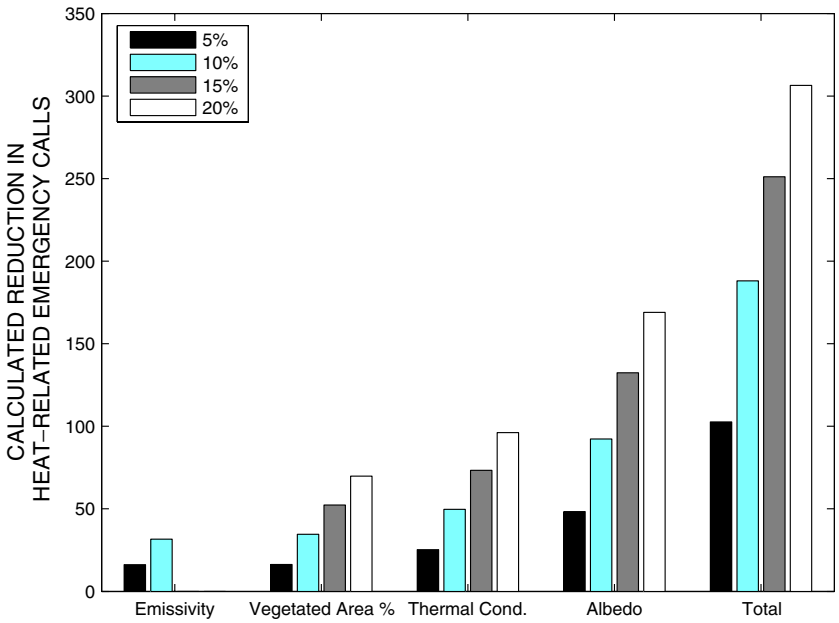


**Fig. 6** Predicted annual reduction in heat-related emergency calls for the city of Phoenix resulting from the four investigated UHI mitigation strategies

## Conclusions with mitigation strategies

The model was run for the 5-year period 2002—2006, for the Phoenix metropolitan region. We extracted only the calculations needed for this analysis, which are the occurrences where there was a heat-related emergency dispatched by the Phoenix Fire Department Regional Dispatch Center. There are 19 extracted calculation sets—2 for the increased emissivity strategy, 4 for the increased albedo strategy, 4 for the increased thermal conductivity strategy, 4 for the increased percentage in vegetated area strategy, 4 for all the strategies in unison, and 1 for the baseline values. Every 24-h average heat index value that occurred when a call was made was inserted into the exponential function (Eq. 7) and given a new predicted heat-related emergency call number. After all occurrences were accounted for, a new total number of predicted emergency calls was recorded for all 19 calculation sets, which is simply the sum of all the predicted heat-related emergency calls for a specific strategy. In order to calculate the actual effect on the decrease in total calls we constructed a percent change (reduction) equation in concert with the

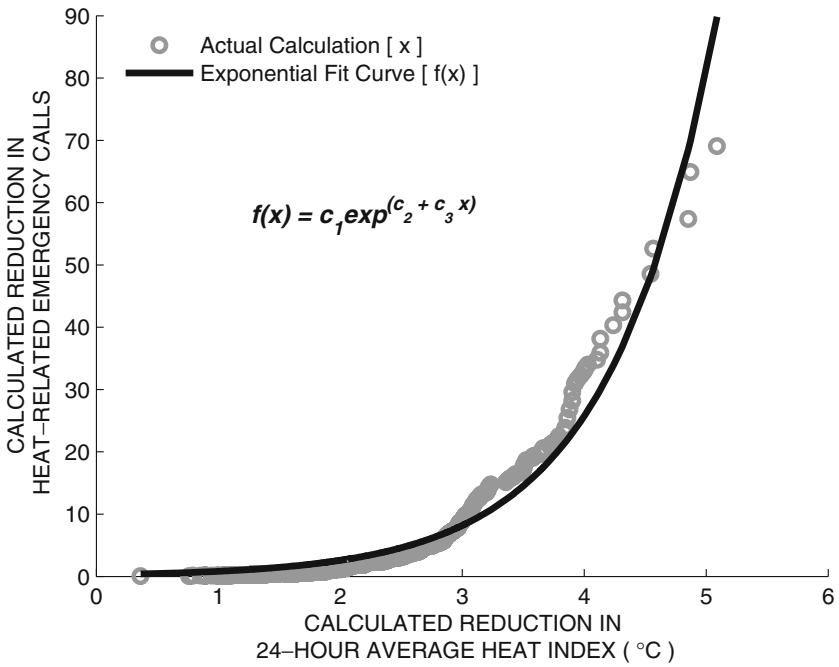


**Fig. 7** Predicted calculated reduction in heat-related emergency calls versus calculated reduction in 24-h average heat index in degrees Centigrade for the city of Phoenix spanning 2002–2006 resulting from all the run sets with $c_1$=9.54, $c_2$=−3.59, and $c_3$=1.14

baseline values calculation set (predicted 3,538 total calls), since the baseline calculation will serve as the predicted total number of calls as calculated by the exponential function. The formulation for the resulting reduction in calls for a particular strategy was taken as follows:

$$\mathrm{RIC} = \frac{\mathrm{BVP} - \mathrm{MSP}}{\mathrm{BVP}} \tag{8}$$

where RIC is the reduction in heat-related emergency calls, BVP is the baseline value prediction and MSP is the mitigation strategy prediction.

Table 7 presents the approximate values for each mitigation strategy's average annual reduction in heat-related emergency calls, and Fig. 6 shows a bar graph of the relative impacts of the different strategies. Increasing albedo results in the highest reduction in heat-related dispatches, while increasing emissivity had the lowest reduction, which is in line with previous results for 24-h average temperatures. The increased thermal conductivity strategy had a larger effect than increasing the percentage of vegetated area strategy, and when we apply all of the strategies together we achieve the largest reduction in calls, which is in qualitative agreement with our earlier analysis.

The model predicts that we can reduce the total of number of calls from 3,186 (over the 5-year period) by 1,530 if we implement the 20% increase for the combined UHI mitigation strategies. Thus, the model showed that the total number of calls can be reduced by almost half if the most aggressive mitigation strategies were deployed in unison. Additionally, by implementing the most passive strategies in unison (all strategies at the 5% increase), the number of calls can be reduced by 515, which is still approximately a 16% from the 3,186 total. These findings show that any strategy listed can have impacts on the number of heat-related emergency calls, which has various sustainable development implications. Furthermore, of the four discussed UHI mitigation strategies, increasing the albedo will lead to the greatest reduction in heat-related emergency calls, increasing the thermal conductivity comes in second, increasing the vegetated area comes in third, and increasing the emissivity comes in last. Concluding our analysis, we would like to show a relationship between the calculated reduction in 24-h average heat index and the calculated reduction in heat-related emergency calls for the entire run set. Figure 7 shows a sound relationship between these two data sets, where their correlation coefficient is $r$=0.78 and best fit was found to be:

$$f(x) = c_1 \exp^{(c_2 + c_3 x)} \tag{9}$$

where $c_1$=9.54, $c_2$=−3.59, and $c_3$=1.14. Equations 7, 8, 9 show the full functional relationship of the model with heat-related calls, which affords policy makers the flexibility of planning with either metric (24-h average heat index or reduction in 24-h average heat index). Lastly, these findings show promise when embarking on these strategies to facilitate the well-being of those impacted by the extreme heat.

In order to be able to run the model for another arid climate such as the urban area of Las Vegas, Nevada, or other regions, practitioners would need to obtain measured data for certain thermophysical constants and dynamic meteorological parameters. These would include the following five thermophysical constants: (1) emissivity (%), (2) albedo (%), (3) volumetric heat capacity (J $m^{-3}$ $K^{-1}$), (4) thermal conductivity (W $m^{-1}$ $K^{-1}$), and (5) the land-cover distribution, like that shown in Table 1. Second, the following seven regional specific dynamic meteorological data would have to be obtained and incorporated into the model: (1) air temperature (K), (2) relative humidity (%), (3) solar irradiation (W $m^{-2}$), (4) wind velocity (m $s^{-1}$), (5) evapotranspiration rate (m $s^{-1}$), and ground/soil temperature (K) at a depth where the temperature does not vary greatly with time. Once the user has the above data they can run the model and/or analyze various mitigation strategies.

**Acknowledgments** This work was supported by the National Center for Environmental Health at the US Centers for Disease Control and Prevention (Contract 30-07184-03 CDC / Task Order 0078), and the National Center of Excellence on SMART Innovations (www.ASUsmart.com) at Arizona State University. H.R.S. gratefully acknowledges the partial support of this work by the National Consortium for Graduate Degrees for Minorities in Engineering and Science, Inc. in the form of a GEM Doctoral Fellowship.

## References

ASHRAE (2004) Handbook of fundamentals. American Society of Heating Refrigeration and Air-Conditioning Engineers, McGraw-Hill, New York

AZMET (2008) http://ag.arizona.edu/azmet/ [accessed Nov. 3, 2008]

Bhardwaj R, Phelan P, Golden J, Kaloush K (2006) An urban energy balance for the Phoenix, Arizona USA Metropolitan Area. 2006 ASME International Mechanical Engineering Congress and Exposition. Chicago, IL, IMECE2006-15308

Cengel AY (2003) Heat transfer: a practical approach. McGraw-Hill, New York

Energy Information Administration [EIA] (2008) http://www.eia.doe.gov/ [accessed Nov. 3, 2008]

Envi-met (2008) http://www.envi-met.com/ [accessed Oct. 7, 2008]

Environmental Protection Agency [EPA] (2001) Cooling our communities. Lawrence Berkeley Laboratory, EPA

Environmental Protection Agency [EPA] (2008) http://www.heatislandmitigationtool.com/ [accessed Oct. 7, 2008]

Golden JS, Kaloush K (2006) Meso-scale and micro-scale evaluations of surface pavement impacts to the urban heat island effects. Int J Pavement Eng 7:37–52

Golden JS, Guthrie P, Kaloush K, Britter R, ES4 (2005) The summertime urban heat island hysteresis lag complexity: applying

thermodynamics, urban engineering and sustainability research. Sustain Eng 158:197–210

Golden JS, Hartz D, Brazel A, Luber G, Phelan PE (2008) A biometeorology study of climate and heat-related morbidity in Phoenix from 2001 to 2006. Int J Biometeorol 52:471–480

Grossman-ClarKe S, Zehnder JA, Stefanov WL, Liu Y, Zoldak MA (2005) Urban modifications in a mesoscale meteorological model and the effects on near surface variables in an arid metropolitan region. J Appl Meteorol 44:1281–1297

Kreyszig E (1999) Advanced Engineering Mathematics. Wiley, New York, pp 1150–1153

Michalakes J, Dudhia J, Gill D, Klemp J, Skamarock W (1998) Design of a next-generation regional weather research and forecast model: towards teracomputing. World Scientific, River Edge, NJ, pp 117–124

Mityakin PL, Pivinskii YE (1980) Properties of quartz-ceramic concrete. Refract Ind Ceram 24:501–505

Pomerantz M, Akbari H, Chen A, Taha H, Rosenfeld AH (1997) Paving materials for heat island mitigation. Ernest Orlando Lawrence Berkeley National Laboratory, LBL-38074

Rosenfeld AH, Akbari H, Bretz S, Fishman B, Kurn DM, Sailor D, Taha H (1995) Mitigation of urban heat island: materials, utility programs, updates. Energy Build 22:255–265

Sailor D, Lu L (2004) A top-down methodology for developing diurnal and seasonal anthropogenic heating profiles for urban areas. Atmos Environ 38:2737–2748

Silva HR, Bhardwaj R, Phelan PE, Golden JS, Grossman-Clarke S (2008) Development of a zero-dimensional mesoscale thermal model for urban climate. J Appl Meteorol Climatol 48:657–668

Stull RB (1999) Meteorology for scientists and engineers. Brooks Cole, Pacific Grove, CA

Taha H, Chang S, Akbari H (2000) Meteorological and air quality impacts of heat island mitigation measures in three U.S. Cities. Lawrence Berkeley National Labortaory, LBNL-44222